JOURNAL OF MATERIALS SCIENCE 35 (2000) 2455–2466

Mechanical modelling of the universal superplastic curve

R. A. VASIN, F. U. ENIKEEV, M. I. MAZURSKI, O. S. MUNIROVA
Institute for Metals Superplasticity Problems, Khalturina, 39, Ufa, 450001, Russia
E-mail: enikeev@anrb.ru

The mechanical response of various combinations of non-linear viscous elements (dashpots) is analysed in this paper. It is assumed that the properties of i-th element can be described by the relation $\sigma_i = K_i \dot{\xi}_i^{m_i}$, where σ_i is the stress, $\dot{\xi}_i$ is the strain rate, K_i and m_i are constants ($0 \leq m_i \leq 1$). Parallel, series and combined combinations are considered. The main object is to find out the potential for various combinations to describe the sigmoidal variation of the flow stress, σ, with the strain rate, $\dot{\xi}$, which is a typical feature of superplastic materials. It is found that elements are connected in parallel as well as elements are connected in series are characterised by non-sigmoidal dependency of the net stress σ on the net strain rate $\dot{\xi}$. At the same time a mixed combination with two elements in parallel connected with a third one in series is shown to describe the sigmoidal curve with reasonable accuracy.

1. Introduction

Structural superplasticity (SP) is observed in ultrafine-grained materials (the average grain size does not exceed 10–15 μm) at high temperatures ($T > 0,4T_m$, where T_m is melting point) and relatively low strain rates (typically 10^{-4}–10^{-1} s^{-1}) [1–6]. The most important characteristic of the superplastic flow is believed to be the high strain rate sensitivity which is usually referred to as

$$\sigma = K\dot{\xi}^m, \tag{1}$$

where K is material constant and m is the so-called strain rate sensitivity index. One can rewrite Equation 1 as follows:

$$\dot{\xi} = C\sigma^n, \tag{1'}$$

where $C = 1/K^n$ and $n = 1/m$.

If one plotted the curve determined by Equation 1 at logarithmic co-ordinates $\log\sigma$–$\log\dot{\xi}$, one could obtained a straight line, the slope of which is equal to m. However, experimental data can not be conventionally fitted by such a straight line, typically one observes the sigmoidal curve [1–6] (see Fig. 1a). That is why it is often said in the literature that Equation 1 is to be treated as a local approximation of the sigmoidal plot which is valid within a sufficiently narrow strain rate interval where the hypothesis $m \cong$ const can be adopted with a reasonable accuracy. In a more general case the slope of the sigmoidal curve, M, is to be taken into consideration in analysing the mechanical response of superplastic materials:

$$M = \frac{\partial \ln\sigma}{\partial \ln\dot{\xi}}. \tag{2}$$

The value of M depends upon strain rate so that the $M(\dot{\xi})$ dependency has a specific dome-like shape (see Fig. 1b). The maximum, M_{max}, corresponds to the optimum strain rate $\dot{\xi}_{opt}$ for a given average grain size and temperature of deformation. The boundaries of the optimum strain rate interval are conventionally found from the empirical condition $M \geq 0.3$ (see Fig. 1b).

The value of the strain rate sensitivity index, m, is believed to be the most important characteristic of a superplastic material. There is a number of reports in the literature where various experimental methods to determine the value of m are described [7–11]. At the same time analysis [12] shows that the value of m depends upon a number of factors: strain, strain rate, structure evolution, deformation mode and type of loading. Therefore this parameter can not be considered as a material constant. In the literature, the difference between m and M is discussed only sometimes, see, for example, [3, 7]. It is to be noted that the dependencies $m(\dot{\xi})$ and $M(\dot{\xi})$ are not the same function, so that one has to keep in this mind when analysing the mechanical response of superplastic materials [13].

Presently the phenomenology of the SP phenomenon is well investigated and many physical models of SP has been suggested in the literature, e.g. [1–6, 14–17]. It is usually assumed that the superplastic deformation is effected by means of the following mechanisms: grain boundary sliding (GBS), diffusion creep (DC) and intragranular slip (IS). Correspondingly, the total plastic strain rate $\dot{\xi}^p$ is often assumed to be as follows:

$$\dot{\xi}^p = \dot{\xi}_{GBS} + \dot{\xi}_{DC} + \dot{\xi}_{IS}. \tag{3}$$

The contribution of each micromechanism, e.g., GBS, is defined as follows $\beta_{GBS} = \dot{\xi}_{GBS}/\dot{\xi}^p$ [6, 18, 19]. It is often assumed that every mechanism of superplastic deformation is characterised by its own value of the strain rate sensitivity index m, e.g., for GBS it is assumed

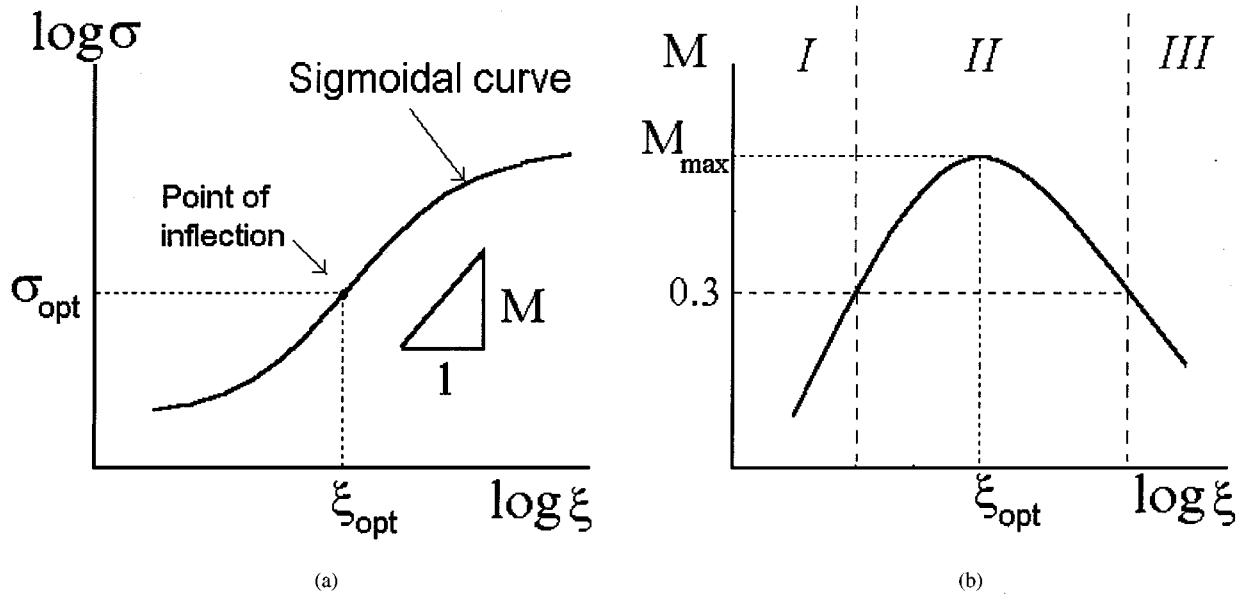

Figure 1 (a) Sigmoidal $\log\sigma - \log\xi$ relationship, and (b) $M(=\partial(\log\sigma)/\partial(\log\xi))$ variation for a superplastic alloy (schematic).

$m_{GBS} \approx 0.5$, for DC it is assumed $m_{DC} \approx 1$, while for IS it is assumed $m_{IS} \approx 0.1$. The resulting value of the strain rate sensitivity index, m, is believed to be determined by interaction of all mechanisms.

Though a number of physical models of SP phenomenon have already been suggested in the literature, it is not yet clearly understood what model (or what combination of micromechanisms) is to be considered as the most appropriate for the experimental data available. It is often assumed [1–6, 14–19] that the contribution of GBS is of its maximum value in the vicinity of the point of inflection of the sigmoidal curve (see Fig. 1a). However, recently a number of reports has been published, see, e.g. [20–24], which are not consistent with this concept.

From the mechanical point of view one can consider Equation 3 as a combination of three non-linear viscous elements (dashpots) which are connected in series. The properties of such a combination may be described by the following equation:

$$\xi^{p} = C_{GBS}\sigma^{n_{GBS}} + C_{DC}\sigma^{n_{DC}} + C_{IS}\sigma^{n_{IS}}, \qquad (4)$$

where $n_{GBS} = 1/m_{GBS}$; $n_{DC} = 1m_{DC}$; $n_{IS} = 1/m_{IS}$ and C_{GBS}, C_{DC} and C_{IS} are material constants. The following question arises then: is it possible to describe the standard sigmoidal curve of SP shown in Fig. 1a by means of Equation 4? Little attention is given to this matter in the literature. If it is not possible to describe the sigmoidal curve by means of an appropriate choice of material constants for Equation 4, then one should modify Equation 4 itself so that it will be possible to describe the sigmoidal variation of the flow stress with strain rate.

We will assume further that the properties of i-th element can be described by the following simplest power relation:

$$\sigma_i = K_i\xi_i^{m_i}, \quad i = 1, 2, \ldots, N, \qquad (5)$$

where σ_i is the stress of i-th element; ξ_i is its strain rate; K_i and m_i are material constants characterising the properties of i-th element ($0 \le m_i \le 1$). Parallel, series and mixed combinations are considered below. The abilities of such combinations to describe the standard superplastic curves shown in Fig. 1 receive primary consideration in our analysis. It is to be emphasised that the physical meaning of the models under consideration will not be taken into account in further analysis. As the value of the strain rate sensitivity index, m, is not equal to the slope of the sigmoidal curve $M(\xi)$, the corresponding theoretical expressions of $m(\xi)$ and $M(\xi)$ functions for all combinations involved are obtained and compared below.

2. The universal superplastic curve

Values of M_{max}, σ_{opt} and ξ_{opt} for different superplastic materials are different (Fig. 2a). But when the same data were plotted in normalised co-ordinates, (M/M_{max}) versus $\log(\xi/\xi_{opt})$, the data points corresponding to the different systems fell on the same curve (Fig. 2b). This 'universal curve' can be described by the empirical Equation [25]

$$\frac{M}{M_{max}} = \exp\left[-a^2\left\{\log\left(\frac{\xi}{\xi_{opt}}\right)\right\}^2\right] \qquad (6)$$

where $a^2 \equiv 0.25$ for a wide range of materials [25].

Substituting Equation 6 at Equation 2 one obtains after integration

$$\log\frac{\sigma}{\sigma_{opt}} = M_{max}\int_0^{\log\frac{\xi}{\xi_{opt}}} \exp[-a^2x^2]\,dx \qquad (7)$$

As Fig. 2b seems to describe the flow behaviour of some superplastic alloys rather well, it is meaningful to check its 'universality' as well as the relevance of the various physical models of superplastic deformation in terms of this curve.

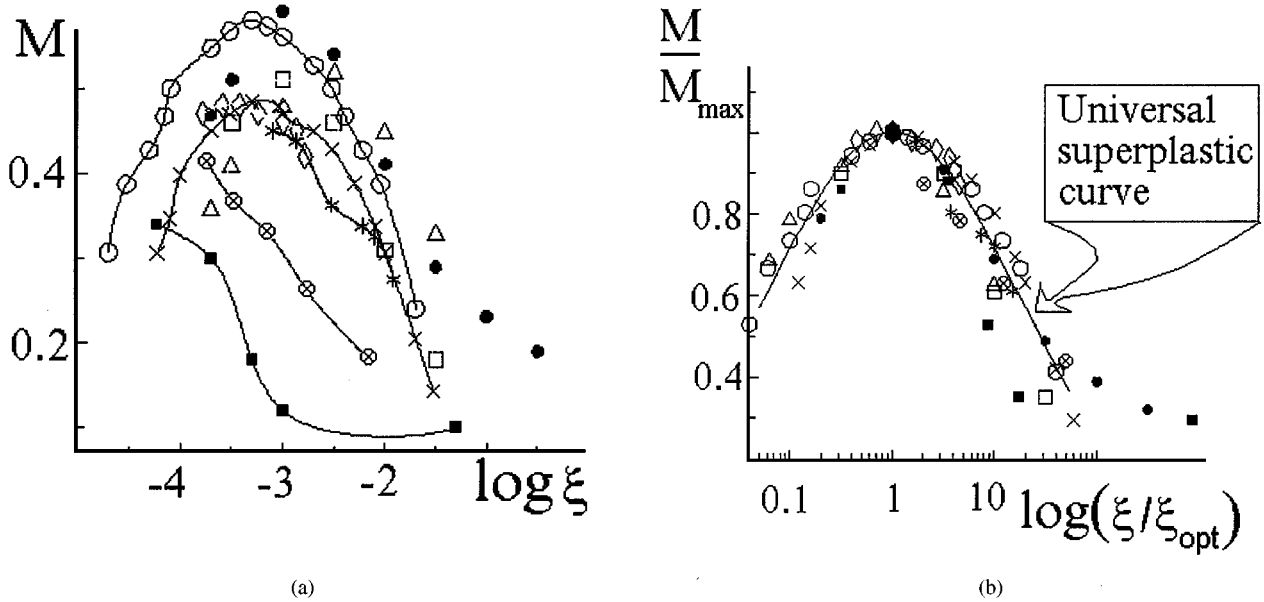

(a) (b)

Figure 2 Experimental dependence of M on strain rate in (a) normal, and (b) normalised co-ordinates [25]: ●●●●—MA21 [6]; ΔΔΔΔ—VT9 [6]; □□□□—0. 12C18Cr10Ni1T [6]; ◇◇◇◇—TiAl [26]; ■■■■—Bi_2O_3 [27]; ⊗⊗⊗⊗—TiC [28]; ◯◯◯◯—5083 [29]; ××××—Ti25Al10Nb3V1Mo [30]; ∗∗∗∗—Ni_3Si [31].

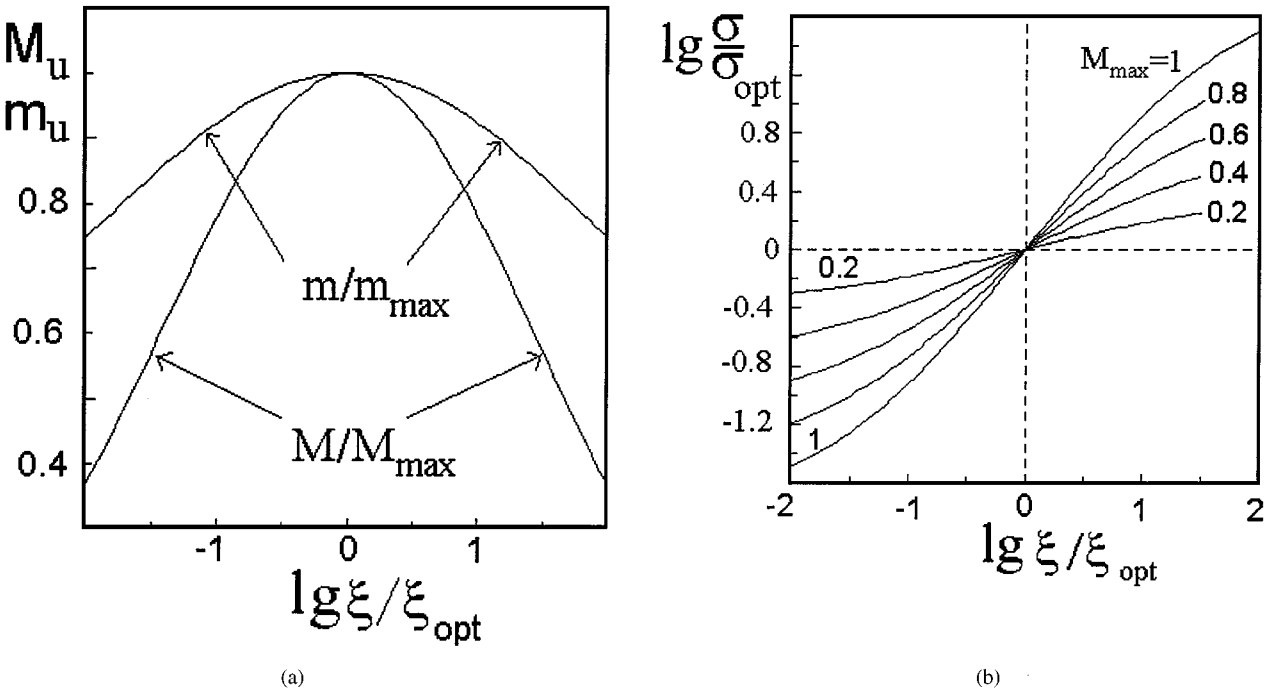

(a) (b)

Figure 3 Universal superplastic curves: (a) $M(\xi)$ and $m(\xi)$ dependencies calculated according to Equations 6 and 7 with $a = 0.5$; (b) Stress–strain rate curves calculated according to Equation 7 with various M_{max} (indicated by the numbers near the curves).

In Fig. 3 the results of calculations in accordance with Equations 6 and 7 are presented. Since the dependencies shown in Fig. 3, are common for a wide range of materials (metals, alloys, ceramics, intermetallic compounds, etc.) it seems to be reasonable to use them in validating the physical models of SP. It is evident that an adequate physical model of the SP phenomenon should acceptably describe the dependencies $M(\xi)$ and $m(\xi)$ shown in Fig. 3.

As it is already mentioned above, the attention of many investigators of the SP phenomenon is directed to the quest of reasonable combinations of elementary micromechanisms of deformation. One can make such searches more effective if one uses one of the standard methods of the mechanics of solids, which is known as mechanical modelling. In accordance with this method each micromechanism can be attributed to a non-linear viscous element, the properties of which are described by Equation 5. Material response can be described by various combinations of such elements. Such combinations are usually known as mechanical models. Each mechanical model is characterised by the number of non-linear viscous elements and the type of connection. We will consider further series, parallel and mixed connection (see Fig. 4).

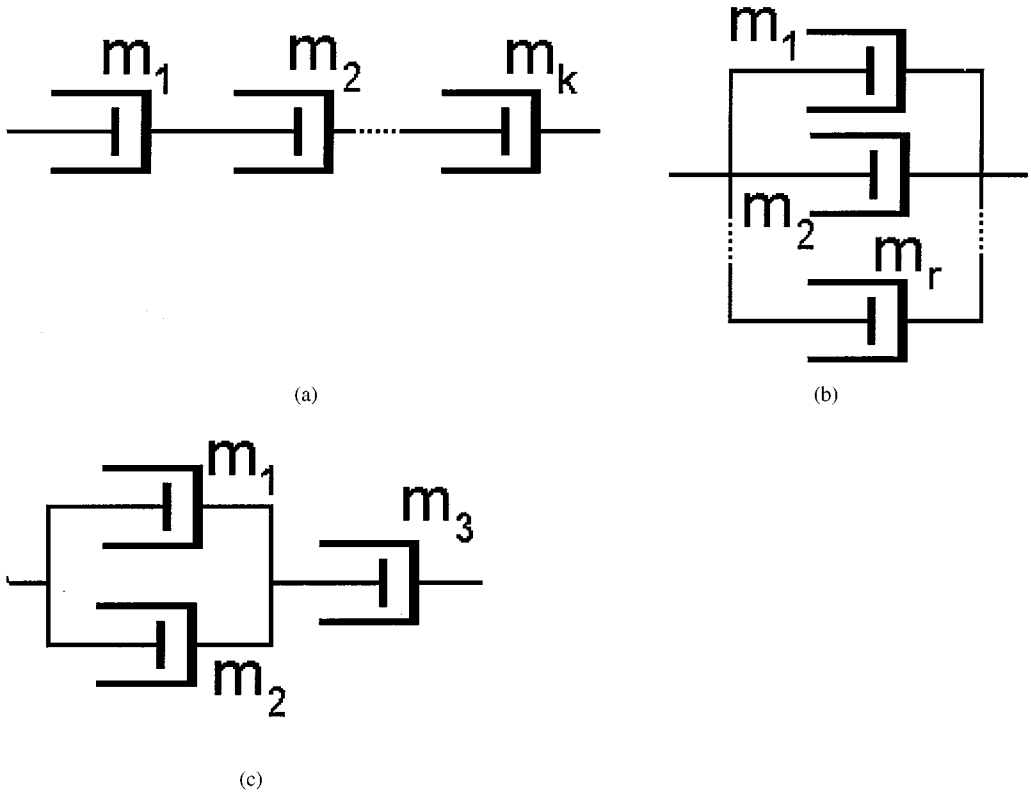

Figure 4 Various combinations of non-linear viscous elements: (a) serial connection; (b) parallel connection; (c) combined connection.

3. Mechanical modelling of the superplastic curve

In this chapter we consider the series, parallel and mixed combinations of the non-linear viscous elements (see Fig. 4).

3.1. Consequent combinations (Fig. 4a)

A number of physical models of the SP phenomenon, known in the literature, can be considered as the consequent joining of the non-linear viscous elements, e.g., [6, 15, 19]. In this case the total strain rate is equal to the sum of elementary strain rates:

$$\xi = \xi_1 + \xi_2 + \cdots + \xi_k = \sum_{i=1}^{k} C_i \sigma^{n_i} = \beta_1 \xi + \beta_2 \xi + \cdots + \beta_k \xi \tag{8}$$

where $\beta_i = \xi_i / \xi$ is the contribution of i-th element. It is evident that $\beta_1 + \beta_2 + \cdots \beta_k = 1$; $0 \le \beta_i \le 1$ $(i = 1, 2, \ldots, k)$. One can see that Equation 8 transfers into Equation 4 when $k = 3$.

Let now $\sigma_s = \sigma(\xi_s)$ be some characteristic value of the stress. We will call this the *reference point*. In particular (but not necessarily) the reference point σ_s, ξ_s may coincide with the point of inflection of the sigmoidal curve σ_{opt}, ξ_{opt} (see Fig. 1a). Let us denote the contributions of various elements at $\xi = \xi_s$ through $\beta_{1s}, \beta_{2s}, \ldots, \beta_{ks}$: $\beta_{is}\xi_s = C_i \sigma_s^{n_i}$ $(i = 1, 2, \ldots, k; \beta_{1s} + \beta_{2s} + \cdots + \beta_{ks} = 1)$. Then one can exclude C_i from Equation 8:

$$\bar{\xi} = \beta_{1s}\bar{\sigma}^{n_1} + \beta_{2s}\bar{\sigma}^{n_2} + \cdots + \beta_{ks}\bar{\sigma}^{n_k} = \bar{\sigma}^{n_c} \tag{8a}$$

where $\bar{\sigma} = \sigma/\sigma_s$ and $\bar{\xi} = \xi/\xi_s$ are normalised stress and strain rate respectively, $n_c = 1/m_c$, where m_c is an effective value of the strain rate sensitivity index, m, for the chain under consideration. It should be mentioned that the contribution β_{is} is of i-th element at $\xi = \xi_s$; is not equal to that at $\xi \neq \xi_s$. It can be shown that

$$\beta_i = \beta_{is} \frac{\bar{\sigma}^{n_i}}{\bar{\xi}} \quad (i = 1, 2, \ldots, k). \tag{9}$$

On the other hand, the introduction of β_{is} leads to the values of C_i being unambiguously determined by the relationships $C_i = \beta_{is}\xi_s/\sigma_s^{n_i}$ $(i = 1, 2, \ldots, k)$. Similarly, introducing C_i unambiguously determines the values of β_{is} by means of the following relations: $\beta_{is} = C_i \sigma_s^{n_i}/\xi_s$ $(i = 1, 2, \ldots, k)$. The slope of the sigmoidal curve is defined as $1/M = \mathrm{d}\log\xi/\mathrm{d}\log\sigma = \mathrm{d}\log\bar{\xi}/\mathrm{d}\log\bar{\sigma}$. It is easy to show that

$$M_c(\xi) = \frac{\beta_{1s}\bar{\sigma}^{n_1} + \beta_{2s}\bar{\sigma}^{n_2} + \cdots + \beta_{ks}\bar{\sigma}^{n_k}}{\beta_{1s}n_1\bar{\sigma}^{n_1} + \beta_{2s}n_2\bar{\sigma}^{n_2} + \cdots + \beta_{ks}n_k\bar{\sigma}^{n_k}}, \tag{10}$$

where $\bar{\sigma} = \bar{\sigma}(\bar{\xi}) = \bar{\xi}^{m_c}$ is the solution of the transcendental Equation 8a, the symbol "c" is used in order to indicate that corresponding m- and M-values refer to the case of serial joining. It may be shown that

$$\lim_{\xi\to 0} M_c(\xi) = \lim_{\xi\to 0} m_c(\xi) = m_{max} = \max_{i=1,2,\ldots,k} m_i; \tag{11a}$$

$$\lim_{\xi\to \infty} M_c(\xi) = \lim_{\xi\to \infty} m_c(\xi) = m_{min} = \min_{i=1,2,\ldots,k} m_i. \tag{11b}$$

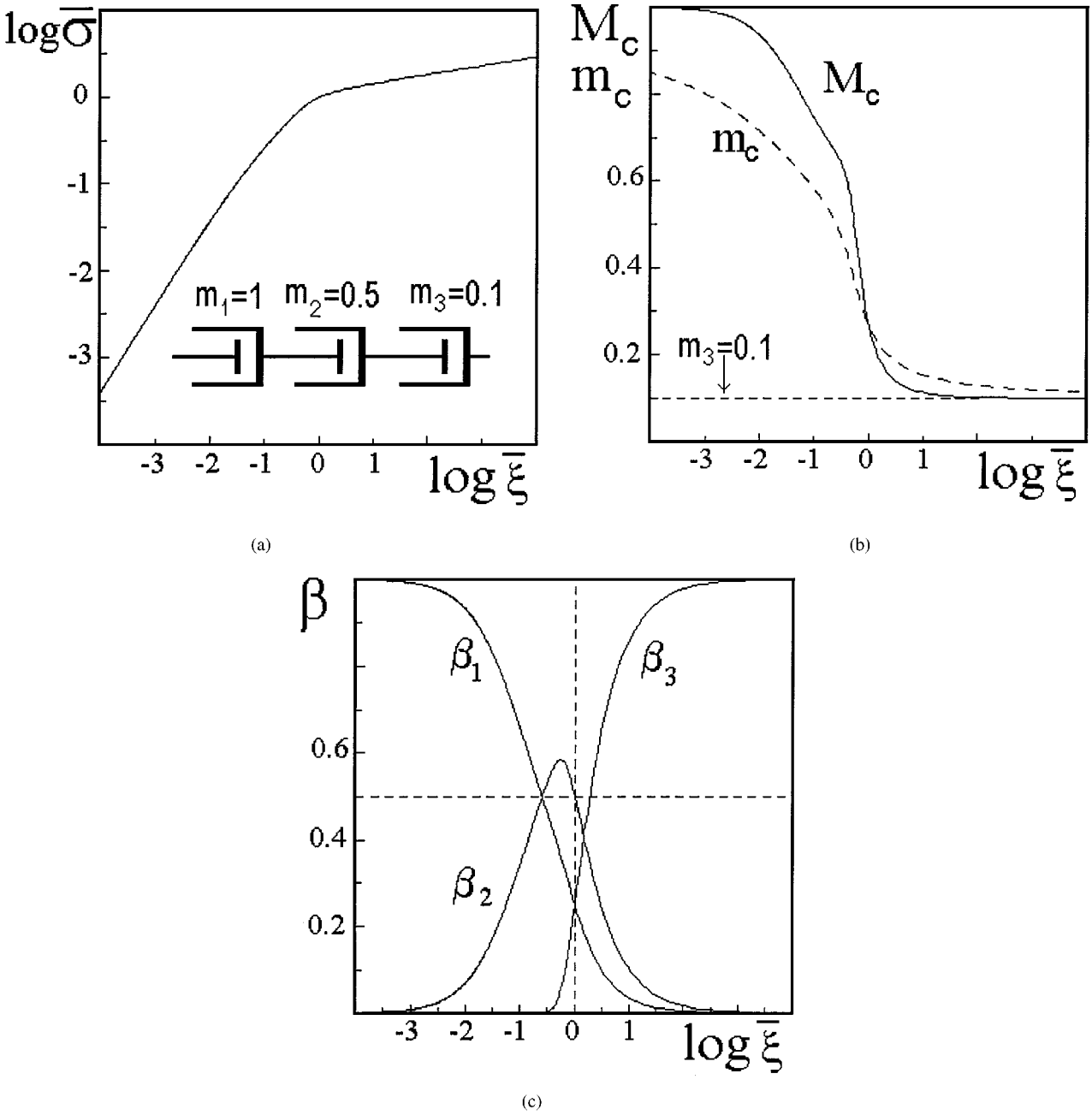

Figure 5 Theoretical dependencies calculated for the serially connected chain with $k=3$, $m_1=1$, $m_2=0.5$, $m_3=0.1$, $\beta_{1s}=0.25$, $\beta_{2s}=0.5$, $\beta_{3s}=0.25$: (a) stress–strain rate curve (Equation 8); (b) $M_c(\xi)$ curve (solid line—Equation 10) and $m_c(\xi)$ curve (dashed line—Equation 8a); (c) contributions β_i (Equation 9).

Thus, at low strain rates ($\xi/\xi_s \to 0$) the values of M_c and m_c tend to m_{max}, while at large ξ ($\xi/\xi_s \to \infty$) they tend to m_{min} (where m_{max} and m_{min} are the maximum and minimum values of m_i for the chain under consideration).

In Fig. 5 the strain rate dependencies for $\bar{\sigma}$ and M_c, m_c and contributions $\beta_i (i=1, 2, 3)$ are presented. One can see in Fig. 5a, that the curve $\log\bar{\sigma} - \log\bar{\xi}$ is convex. The values of M_c and m_c decrease monotonically with ξ (Fig. 5b). At low ξ the element with maximum m ($m_{max}=m_1=1$) dominates, so that $\beta_1 \to 1$ with $\xi \to 0$ (see Fig. 5c). At large ξ the element with minimum m ($m_{min}=m_3=0.1$) makes the main contribution, so that $\beta_3 \to 1$ with $\xi \to \infty$ (see Fig. 5c). The contribution of the non-linear viscous element $m_2=0.5$ is of its maximum value for intermediate strain rates (Fig. 5c).

The following natural question arises then: is it possible to describe the sigmoidal superplastic curve by connecting additional elements to the chain (Fig. 3a) and by varying their relative contributions β_{is}? We have fulfilled a number of additional numerical experiments in order to answer this question. We have varied the number of elements at the chain (the calculations were fulfilled for $k=2, 3, 4, 5$) as well as their relative contributions $\beta_{1s}, \beta_{2s}, \ldots, \beta_{ks}$ and strain rate sensitivity indexes $m_1, m_2, \ldots, m_k$. The results of calculations show that the values of $M_c(\xi)$ and $m_c(\xi)$ decrease monotonically from $m_{max}=\max\{m_i\}$ to $m_{min}=\min\{m_i\}$ for all cases considered. Thus, we have concluded that the consequent combinations of elements are always characterised by convex (that is, non-sigmoidal) curve $\log\bar{\sigma} - \log\bar{\xi}$ for arbitrary $m_i \geq 0$

and $\beta_{is} \geq 0$ ($i = 1, 2, \ldots, k$). Hence, the physical models based upon the hypothesis of additivity (similar to Equation 4) *are not capable of describing the sigmoidal curve of SP*. That is why it is of interest to consider other possible ways to combine the non-linear viscous elements into the mechanical model.

3.2. Parallel combinations (Fig. 4b)

In this case each element makes a contribution to the total stress. For example, for the case when two non-linear viscous elements are connected in parallel one has

$$\sigma = K_1 \dot{\xi}^{m_1} + K_2 \dot{\xi}^{m_2}. \tag{12}$$

One can find a number of physical models in the literature that may be presented as a parallel combinations of non-linear viscous elements. For instance, the so-called "threshold stress" can be taken into consideration in describing the mechanical response of superplastic materials, see, e.g. [32]. In this case one can assume $m_1 \to 0$.* On the other hand, recently it was reported [33] that Equation (12) (with non-zero m_1 and m_2) may be successfully applied to superplastic aluminium 7075 and Al-4%Ti alloys (the value of the coefficient of correlation exceeds 0.999 for all experimental curves). Expressions similar to Equation (12) are widely used in the mechanics of composites; it may be used in order to simulate the rheological behaviour of two-phase titanium alloys as well.

For the case when r non-linear viscous elements are connected in parallel, we have:

$$\sigma = \sum_{i=1}^{r} K_i \dot{\xi}^{m_i} = \alpha_1 \sigma + \alpha_2 \sigma + \cdots + \alpha_r \sigma, \tag{13}$$

where $\alpha_i = \sigma_i / \sigma$ is the contribution of i-th element to the total stress. Let, for some reference point $\sigma_q = \sigma(\xi_q)$, the contributions be equal to $\alpha_{1q}, \alpha_{2q}, \ldots, \alpha_{rq}$ respectively, then one can rewrite Equation 13 as follows

$$\bar{\sigma} = \sum_{i=1}^{r} \alpha_{iq} \bar{\xi}^{m_i} = \bar{\xi}^{m_p}, \tag{14}$$

where $\bar{\sigma} = \sigma / \sigma_q$, $\bar{\xi} = \xi / \xi_q$, m_p is an effective value of the strain rate sensitivity index, m, for a combination under consideration. The contributions of elements depends upon strain rate. One can obtain that

$$\alpha_i = \frac{\sigma_i}{\sigma} = \alpha_{iq} \frac{\bar{\xi}^{m_i}}{\bar{\sigma}}, \quad i = 1, 2, \ldots, r, \tag{15}$$

where $\bar{\xi}$ is the solution of the transcendental Eq. (14). Substituting Equation 14 into Equation 2 we obtain

$$M_p = \frac{\alpha_{1q} m_1 \bar{\xi}^{m_1} + \alpha_{2q} m_2 \bar{\xi}^{m_2} + \cdots + \alpha_{rq} m_r \bar{\xi}^{m_r}}{\alpha_{1p} \dot{\xi}^{m_1} + \alpha_{2q} \dot{\xi}^{m_2} + \cdots + \alpha_{rq} \dot{\xi}^{m_r}}, \tag{16}$$

* It should be noted, that for the limiting case $m_1 \to 0$ the following uncertainty takes place: if at $\xi \neq 0$ and $m_1 \to 0$ the value of $\sigma \to K_1 \neq 0$, then at $\xi \equiv 0$ when $m \to 0$ the flow stress $\sigma \equiv 0$.

It may be shown that

$$\lim_{\xi \to 0} M_p(\xi) = \lim_{\xi \to 0} m_p(\xi) = m_{\min} = \min_{i=1,2,\ldots,r} m_i; \tag{17a}$$

$$\lim_{\xi \to \infty} M_p(\xi) = \lim_{\xi \to \infty} m_p(\xi) = m_{\max} = \max_{i=1,2,\ldots,r} m_i. \tag{17b}$$

Thus, at low strain rates ($\xi / \xi_q \to 0$) the values of M_p and m_p tend to $m_{\min}$, while at large ξ ($\xi / \xi_p \to \infty$) they tend to $m_{\max}$ (where $m_{\min}$ and $m_{\max}$ are the minimum and maximum values of m_i at the mechanical model under consideration).

In Fig. 6 the theoretical strain rate dependencies of σ, m_p- and M_p-values are presented. One can see in Fig. 6a, that the curve $\log \bar{\sigma} - \log \bar{\xi}$ is concave. The values of M_p and m_p increase monotonically with ξ (Fig. 6b). At low ξ the element with minimum m ($m_{\min} = m_3 = 0.1$) dominates, so that $\alpha_3 \to 1$ with $\xi \to 0$ (see Fig. 6c). At large ξ the element with maximum m ($m_{\max} = m_1 = 1$) makes the main contribution, so that $\alpha_1 \to 1$ with $\xi \to \infty$ (see Fig. 5c). The contribution of the non-linear viscous element $m_2 = 0.5$ is at its maximum value for intermediate strain rates (Fig. 6c).

The following natural question arises then: is it possible to describe the sigmoidal curve by connecting additional elements to the model shown in Fig. 4b and by varying their relative contributions α_{iq}? We have fulfilled a number of additional numerical experiments in order to answer this question. We have varied the number of elements at the model (the calculations were fulfilled for $r = 2, 3, 4, 5$) as well as their relative contributions $\alpha_{1q}, \alpha_{2q}, \ldots, \alpha_{rq}$ and strain rate sensitivity indexes $m_1, m_2, \ldots, m_r$. The results of calculations show that the values of $M_p(\xi)$ and $m_p(\xi)$ increase monotonically from $m_{\min} = \min\{m_i\}$ to $m_{\max} = \max\{m_i\}$ for all cases considered. Thus, we have concluded that the parallel combinations of non-linear viscous elements are always characterised by a concave (that is, non-sigmoidal) $\log \bar{\sigma} - \log \bar{\xi}$ curve for arbitrary $m_i \geq 0$ and $\alpha_{iq} \geq 0$ ($i = 1, 2, \ldots, r$). Hence, the physical models based upon the hypothesis of simple additivity of the stresses due to different mechanisms (similar to Eq. 12) *are not capable of describing the sigmoidal curve of SP*.

3.3. Mixed combinations (Fig. 4c)

If one compares Figs 5b and 6b, one could conclude that series and parallel connection are characterised by monotonic dependencies $M(\log \xi)$ and $m(\log \xi)$. Actually, the $M_c(\log \xi)$ and $m_c(\log \xi)$ plots are decreasing ones while $M_p(\log \xi)$ and $m_p(\log \xi)$ curves are increasing ones. Hence, one can expect that the mixed combination allows to give some intermediate non-monotonic dependencies of $m(\log \xi)$ and $M(\log \xi)$. There are only a few examples in the literature where such mixed combinations are considered. Zehr and Backofen [34] have considered a mixed combination in order to describe the mechanical response of the superplastic lead–tin eutectic alloy. Recently Perevezentcev *et al.* have suggested a new physical model of the SP phenomenon [14], which describes the sigmoidal variation of σ with ξ. This model is rather cumbersome and so it is not an easy task to proceed using all the calculations presented

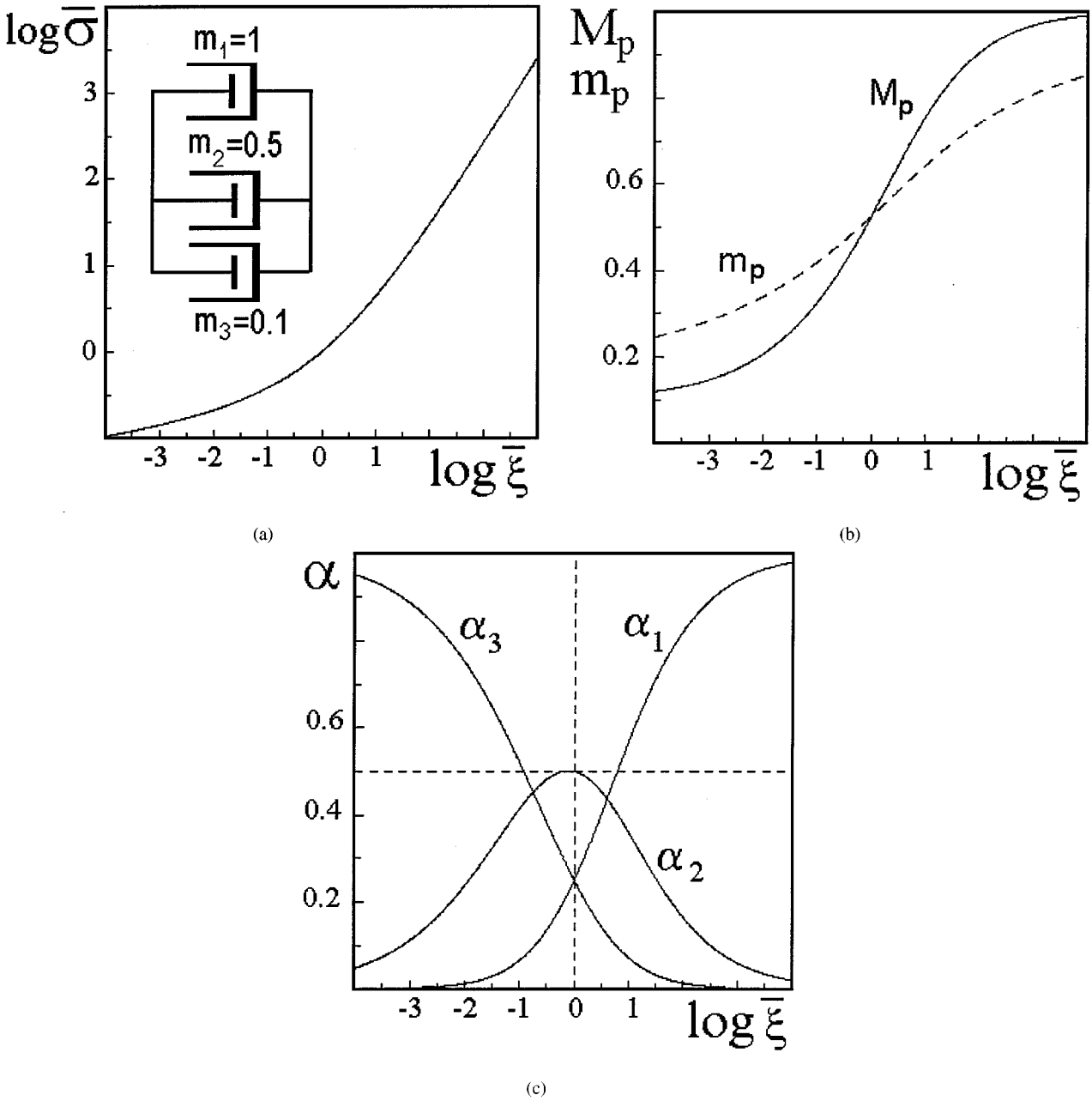

Figure 6 Theoretical dependencies calculated for the parallel combination of non-linear viscous elements with $r = 3$, $m_1 = 1$, $m_2 = 0.5$, $m_3 = 0.1$, $\alpha_{1q} = 0.25$, $\alpha_{2q} = 0.5$, $\alpha_{3q} = 0.25$: (a) stress–strain rate curve (Equation 14); (b) $M_p(\xi)$ curve (solid line—Equation 16) and $m_p(\xi)$ curve (dashed line—Equation 14'); (c) contributions α_i (Equation 15).

in [14]. Nevertheless, proceeding from a number of other publications of Perevethentcev *et al.* one can conclude that they are using the principle of mixed connection in summing the strain rates corresponding to different micromechanisms. Such an approach enables them to describe the experimental sigmoidal curve for titanium alloy Ti-6Al-4V, which has been reported by Ghosh [35]. That is why it is of interest to consider other possible ways to combine the non-linear viscous elements into the mechanical model.

Let us consider the mixed combination consisting of three elements (Fig. 4c). The behaviour of this combination is described by the following equations:

$$\sigma = K_1\xi_1^{m_1} + K_2\xi_2^{m_2} = K_3\xi_3^{m_3},$$
$$\xi_1 = \xi_2, \quad \xi = \xi_1 + \xi_3, \tag{18}$$

where $\xi_i (i = 1, 2, 3)$ are the strain rates of i-th element; K_i, m_i $(i = 1, 2, 3)$ are the material constants. One can write the following relationships. For some reference point $\sigma = \sigma(\xi_0)$ we obtain

$$\sigma_0 = K_1\xi_{10}^{m_1} + K_2\xi_{20}^{m_2} = \alpha_{10}\sigma_0 + \alpha_{20}\sigma_0,$$
$$\xi_0 = \xi_{10} + \xi_{30} = \beta_{10}\xi_0 + \beta_{20}\xi_0. \tag{19}$$

Taking into account Equation 19 one can find from Equation 18:

$$\bar{\sigma} = \frac{\alpha_{10}}{\beta_{10}^{m_1}}(\bar{\xi} - \bar{\xi}_3)^{m_1} + \frac{\alpha_{20}}{\beta_{20}^{m_2}}(\bar{\xi} - \bar{\xi}_3)^{m_2} = \frac{1}{\beta_{30}^{m_3}}\bar{\xi}_3^{m_3} = \bar{\xi}^{m_m}, \tag{20}$$

where $\bar{\sigma} = \sigma/\sigma_0$, $\bar{\xi} = \xi/\xi_0$ and it is taken into account that $\bar{\xi}_1 = \bar{\xi}_2 = \bar{\xi} - \bar{\xi}_3$. It is easy to see that for a given

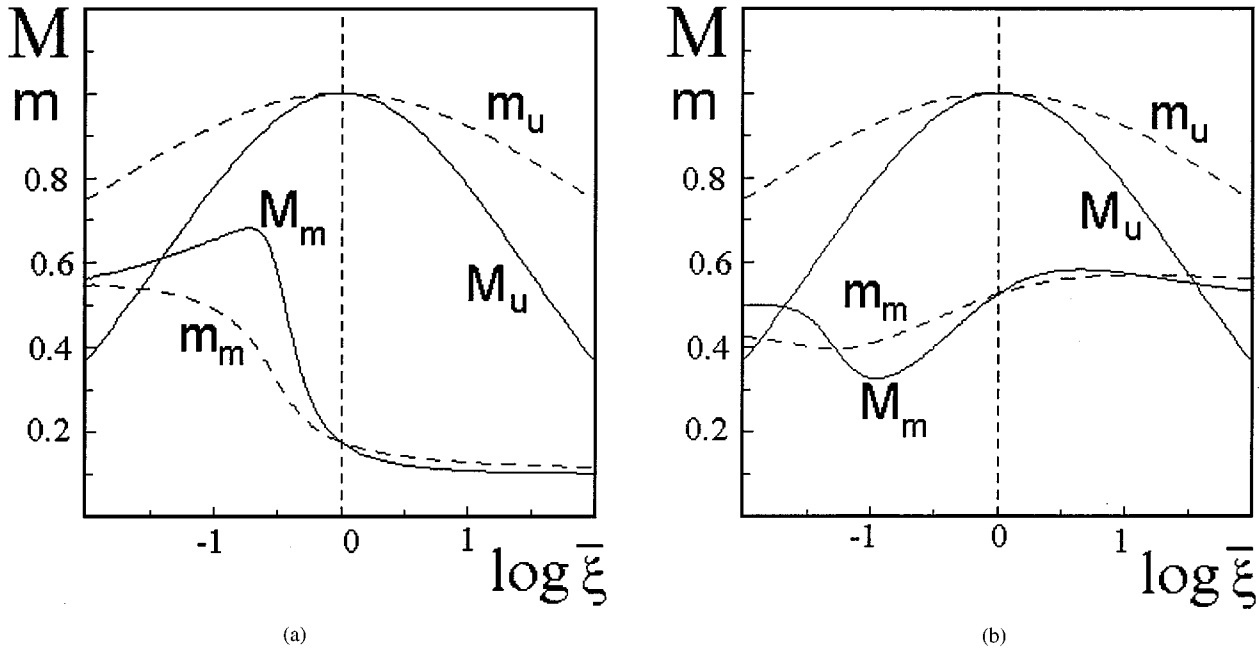

Figure 7 Strain rate dependencies of M-values (solid lines) and m-values (dashed lines) calculated in accordance with Equations 6, 7, 20 and 21 with two different sets of material constants: (a) $m_1 = 1$; $m_2 = 0.5$; $m_3 = 0.1$ $\alpha_{10} = 0.5$; $\beta_{10} = 0.5$ (M_m and m_m-curves); (b) $m_1 = 1$; $m_2 = 0.1$; $m_3 = 0.5$ $\alpha_{10} = 0.5$; $\beta_{10} = 0.5$ (M_m and m_m-curves). M_u and m_u-curves have been calculated with $a = 0.5$ and $M_{max} = 1$.

value of the strain rate ξ Equation 20 represents a transcendental equation as to the unknown function $\bar{\xi}_3$. The value of M for a mixed model may be found as follows:

$$\frac{1}{M_m(\xi)} = \frac{\bar{\xi}_3}{m_3\xi} + \frac{\bar{\xi}_3^{m_3}}{\beta_{30}^{m_3}} \frac{1 - \bar{\xi}_3/\bar{\xi}}{\bar{\alpha}_{10} m_1 (\xi - \xi_3)^{m_1} + \bar{\alpha}_{20} m_2 (\xi - \xi_3)^{m_2}}, \tag{21}$$

where $\bar{\alpha}_{i0} = \alpha_{i0}/\beta_{i0}^{m_i}$ $(i = 1, 2)$, and $\bar{\xi}_3$ is the solution of Equation 20. One can show that

$$\lim_{\alpha \to 0} M_m(\bar{\xi}) = M_c; \quad \lim_{\beta_3 \to 0} M_m(\bar{\xi}) = M_p;$$
$$\lim_{\bar{\xi}_3 \to \xi} M_m(\bar{\xi}) = m_3 \tag{22}$$

The results of calculations in accordance with Equations 20 and 21 are presented in Fig. 7. One can see in Fig. 7, that the corresponding $M_m(\log \xi)$ dependencies has non-monotonic character. However, there is a considerable difference between $M_m(\log \xi)$ plots and the corresponding universal dependency $M_u(\log \xi)$. That is why we have fulfilled a number of additional calculations with various values of material constants m_1, m_2, m_3, α_{10}, and β_{10}. As a result, good agreement between $M_m(\log \xi)$ and $M_u(\log \xi)$ curves as well as between $m_m(\log \xi)$ and $m_u(\log \xi)$ curves has been found (see Fig. 8). It is to be noted that the set of constants enabling one to describe adequately the universal superplastic curves is not the only possible one. One can find a number of other sets in Table I. The last column of Table I includes the standard mean square deviation Δ for the results of calculation from the universal superplastic curve shown in Fig. 2b. It is evident that one can find some possible sets of material constants describing the universal superplastic curves with a reasonable accuracy.

TABLE I Sets of material constants for Equations 20 and 21 allowing one to describe the universal superplastic curve shown in Fig. 2b

m_1	m_2	m_3	α_{10}	α_{20}	β_{10}	β_{20}	Δ
1	0,18	0,26	0,94	0,06	0,9999	0,0001	0,05
1	0,1	0,46	0,96	0,04	0,97	0,03	0,05
1	0,4	0,25	0,87	0,13	0,9999	0,0001	0,09
1	0,3	0,25	0,90	0,10	0,9999	0,0001	0,06
1	0,33	0,25	0,88	0,12	0,9999	0,0001	0,07
1	0,2	0,5	0,94	0,06	0,92	0,08	0,08

Zehr and Backofen have applied a mixed mechanical model to eutectic lead–tin alloy [34]. The values of the material constants K_i and m_i have been determined in [34] empirically from the experimental sigmoidal curves. The results obtained in [34] are incorporated into Table II. In order to use these data let us substitute Equation 18 at Equation 2. Then we obtain after some transforms:

$$M_{ZB} = \frac{\left[m_1 K_1 \xi_1^{m_1} + m_2 K_2 \xi_2^{m_2}\right] \frac{\xi}{\xi - \xi_1} m_3}{m_1 K_1 \xi_1^{m_1} + m_2 K_2 \xi_2^{m_2} + \frac{\xi}{\xi - \xi_1} m_3 K_3 (\xi - \xi_1)^{m_3}} \tag{23}$$

where ξ_1 is the solution of the following transcendental equation:

$$\sigma = K_1 \xi_1^{m_1} + K_2 \xi_1^{m_2} = K_3 (\xi - \xi_1)^{m_3} \tag{24}$$

The results of calculations in accordance with Equations 23 and 24 are presented in Fig. 9. The values of m_i and K_i $(i = 1, 2, 3)$ used in calculations have been taken from Table II.

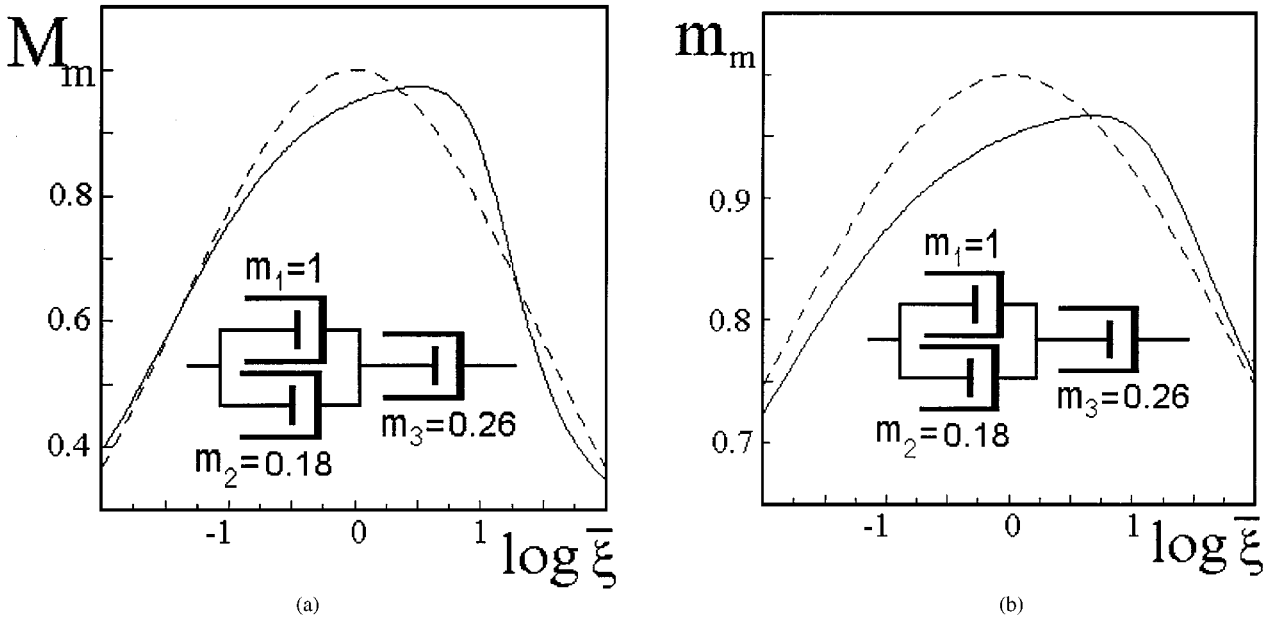

Figure 8 Strain rate dependencies of M-value (a) and m-value (b) for a mixed combination, calculated in accordance with Equations 20 and 21 with $m_1 = 1$; $m_2 = 0.18$; $m_3 = 0.26$ $\alpha_{10} = 0.94$; $\beta_{10} = 0.9999$. For the sake of comparison the corresponding universal curves calculated in accordance with Equations 6 and 7 with $M_{max} = 1$ are presented by dashed lines.

TABLE II Material constants for Zehr–Backofen model [34]

Material	d_0 (μm)	T (°C)	T/T_m	Element's properties (units: lb, in, sec) K_1	m_1	K_2	m_2	K_3	m_3
Pb-Sn	2,0	26	0,65	$6{,}70 \times 10^5$	1	$1{,}15 \times 10^4$	0,33	$1{,}27 \times 10^4$	0,18
[34]	3,1			$2{,}50 \times 10^6$		$2{,}23 \times 10^4$	0,33	$2{,}26 \times 10^4$	0,24
Pb-Sn	2,0	25	0,65	$4{,}20 \times 10^6$	1	$1{,}11 \times 10^4$	0,33	$1{,}9 \times 10^4$	0,21
[35]									
Pb-Sn	2,2	25	0,65	$1{,}65 \times 10^6$	1	$1{,}27 \times 10^4$	0,34	$1{,}68 \times 10^4$	0,25
[36]	4,1			$1{,}06 \times 10^7$		$8{,}47 \times 10^3$	0,28	$2{,}2 \times 10^4$	0,25
Al–Cu	2,3	520	0,97	$2{,}2 \times 10^5$	1	$2{,}63 \times 10^3$	0,33	$1{,}17 \times 10^4$	0,25
[37]	7,7			$2{,}46 \times 10^6$		$2{,}77 \times 10^2$	0,11	$3{,}54 \times 10^4$	0,39

It is pertinent to note that for the case when all non-linear viscous elements contained in the mechanical model under consideration have the same value of the strain rate sensitivity index (that is, $m_1 = m_2 = \cdots = m_0$) then independently of the type of connection the following relationships take place: $M = m = m_0$. This fact is a consequence of Equations 8a, 10, 14, 16, 20 and 21.

4. Discussion

The results obtained enable us to conclude that for the case of serial (Fig. 4a) or parallel (Fig. 4b) connection, the resulting $\log\sigma$–$\log\xi$ curve are not sigmoidal irrespective of the number of elements contained in the mechanical model under consideration. At the same time the mechanical model with mixed connection (Fig. 4c) enables one to describe adequately the universal sigmoidal curve shown in Fig. 2b.

Recently Padmanabhan and Schliepf have presented an analysis of the boundary sliding process [16], which leads to new model for GBS controlled optimal structural SP. A numerical procedure that allows the unambiguous determination of the material constants of this model has been presented and validated by analysing the experimental data pertaining to a few systems in [38]. It was shown that this method allows the determination of the material constants with a limited number of experimental points. A comparison of the predictions with the experimental results shows that this model describes optimal superplastic flow (Regions I and II up to the point of inflection in the sigmoidal $\log\sigma - \log\xi$ curve) accurately. The shape of the universal M-curve on the left hand side of ξ_{opt} is similar to that of the theoretical curves calculated within the framework of Padmanabhan–Schliepf model for different alloys (see Fig. 10). The curves actually coincide (true universal curves) when the (T/T_m) ratios are similar. But the shapes are different on the right hand side of ξ_{opt}. It was found in [38] that the mechanical analogue of Padmanabhan–Schliepf model of the SP phenomenon [16] includes two dashpots (one of which is Newtonian viscous) in series connected to a constant stress term in parallel (see Fig. 10).

It was established in [38] that a 'universal curve' for superplastic flow exists *provided* the (M/M_{max}) vs.

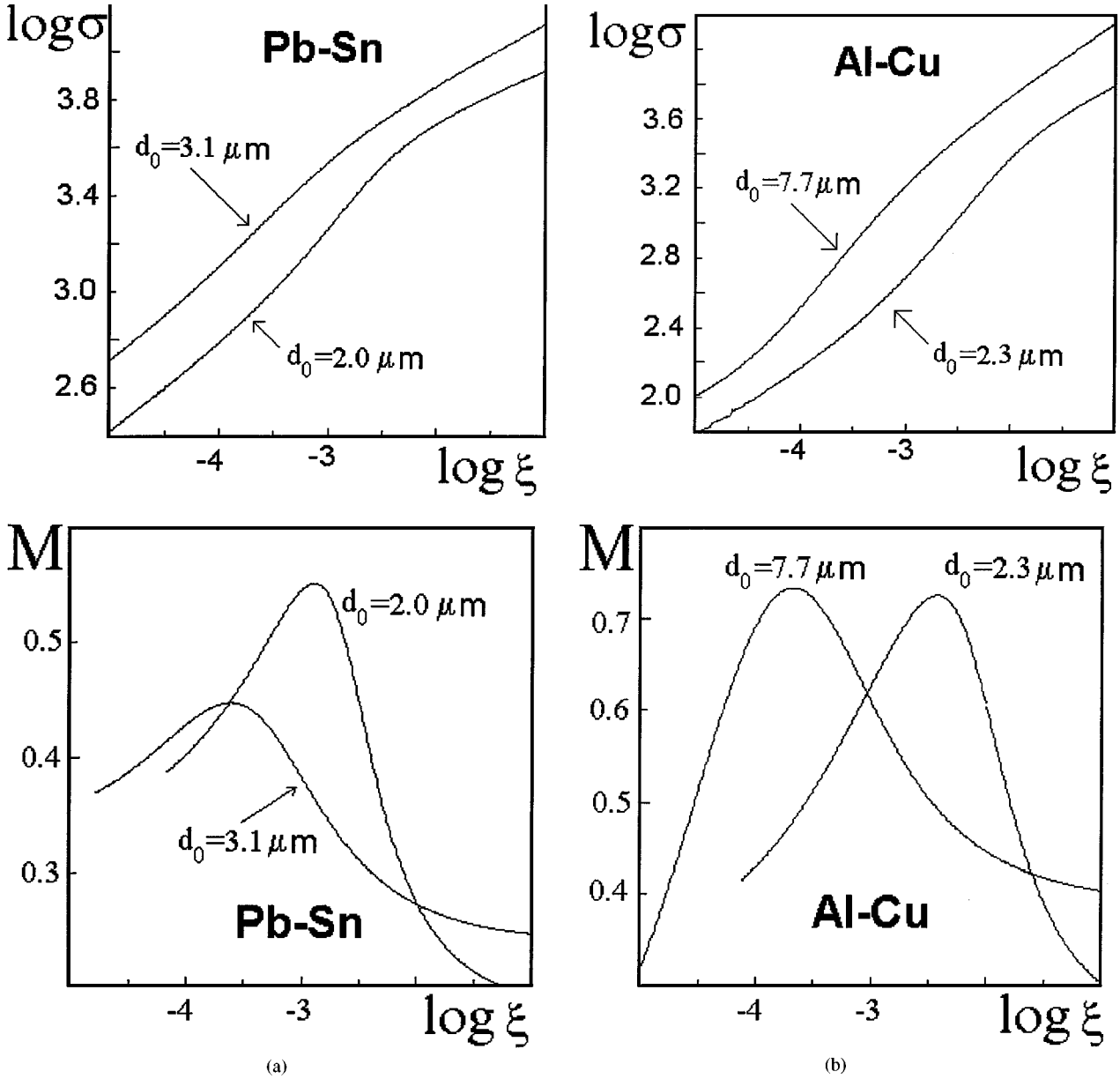

Figure 9 Sigmoidal superplastic curves and corresponding dependencies of their slopes M on the strain rate calculated in accordance with Equations 23 and 24 for eutectic alloys lead–tin (a) and aluminium–copper (b).

$\log(\xi/\xi_{opt})$ plot is made at constant (T/T_m) ratio. In other words, the value of the parameter 'a' at the right side of Equations 6 and 7, in general, depends upon temperature. Typical values of 'a' according to [38] turned out to be of about 0.5–0.7 for a number of aluminium-base alloys. We have fulfilled a number of additional calculations with $a = 0.7$. It was found that mixed combinations allows one to describe the corresponding universal curves with $a = 0.7$ as well (see Fig. 11). We have reported earlier some results of the calculations similar to above considered [39]. In this work the value of parameter 'a' in Equation 6 has been occasionally taken equal to 0.25 and a good agreement was found for the set of material constants $m_1 = 1$; $m_2 = 0.2$; $m_3 = 0.5$, $\alpha_{10} = 0.99$, $\beta_{10} = 0.99$.

It is to be emphasized that the narrowing of the optimum strain rate interval (the contraction of Region II in Fig. 1b) with temperature of deformation is a typical experimental fact. Unfortunately, little attention is given to this in the literature. At the same time the contraction of Region II with T is as universal a fact for the phenomenology of the SP phenomenon as the sigmoidal variation of the flow stress with strain rate. That is why it is very important to keep in mind this circumstance when constructing adequate models of the SP phenomenon. Empirically, the narrowing of Region II with T can be described by use of Equations 6 or 7 where the value of 'a' depends upon T (see Fig. 11). It is pertinent to note that the physical reasons for existence of such phenomenon can be clearly explained within the framework of the new concept of the SP phenomenon, which is developed in [24].

The results obtained in the present work indicate that there is a problem in taking into account the simultaneous action of different deformation mechanisms. It is not yet clear what kind of summation is to be used in doing so. For example, one can use the additivity of the strain rates corresponding to different

micromechanisms similar to Equation 4. In this case the stress is assumed to be the same for all micromechanisms involved while each of them contributes to the net value of the strain rate. On the contrary, it is possible to assume that the total strain rate is the same for all micromechanisms while each of them contributes to the total stress and so use Equation 13 in order to describe the net response of a superplastic material. It is possible to consider some intermediate situations as well (e.g., mechanical models shown in Figs 4c and 10).

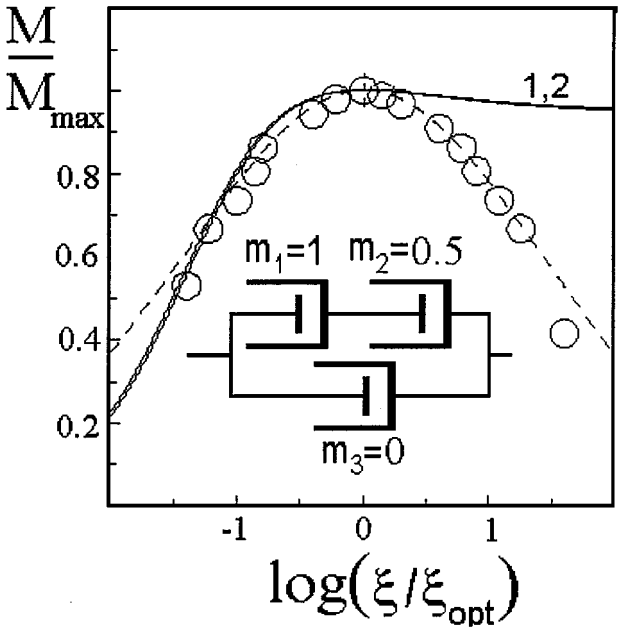

Figure 10 Mechanical analogue of the Padmanabhan–Schliepf model and theoretical (M/M_{max}) vs. $\log(\xi/\xi_{opt})$ plots at comparable (T/T_m) ratio for the following alloys (solid lines) [38]: (1) Zn-22%Al, 503 K, $(T/T_m) = 0.918$; (2) Supral alloy, 743 K, $(T/T_m) = 0.911$. ○○○○ Al5083 deformed at $(T/T_m) = 0.922$ [29]. The original 'universal curve' corresponding to $a = 0.5$ is also shown by dashed line.

References

1. J. W. EDINGTON, K. N. MELTON and C. P. CUTLER, *Progress in Materials Science* **21** (1976) 63.
2. T. G. LANGDON, *Metal. Trans.* **13A** (1982) 689.
3. K. A. PADMANABHAN and J. J. DAVIES, "Superplasticity," (Springer-Verlag, Berlin, Germany, 1980) p. 314 c.
4. J. PILLING and N. RIDLEY, "Superplasticity in Crystalline Solids," The Institute of Metals (The Camelot Press, London, 1989).
5. O. D. SHERBY and J. WADSWORTH, *Progr. In Mat. Sci.* **33** (1989) 169.
6. O. A. KAIBYSHEV, "Superplasticity in Alloys, Intermetallides and Ceramics," (Springer–Verlag, Berlin, Heidelberg, 1992) p. 317.
7. J. HEDWORTH and M. J. STOWELL, *J. Mater. Sci.* **6** (1971) 1061.
8. F. U. ENIKEEV and M. I. MAZURSKI, *Scripta Metall.* **32** (1995) 1.
9. R. A VASIN, F. U. ENIKEEV and M. I. MAZURSKI, *Mater. Sci. Eng.* **A224** (1997) 131.
10. F. U. ENIKEEV and A. A. KRUGLOV, *Int. J. Mech. Sci.* **37** (1995) 473.
11. R. A VASIN, F. U. ENIKEEV and M. I. MAZURSKI, *J. Mater. Sci.* **33** (1998) 1099.
12. F. U. ENIKEEV, *Mater. Sci. Forum* **243–245** (1997) 77.
13. R. A VASIN, F. U. ENIKEEV and M. I. MAZURSKI, *Mater. Sci. Eng.* **255** (1998) 169.
14. V. N. PEREVEZENTSEV, V. V. RYBIN and V. N. CHUVIL'DEEV, *Acta Metall. Material.* **40** (1992) 887.
15. A. K. GHOSH, *Mater. Sci. Forum* **170–172** (1994) 39.
16. K. A. PADMANABHAN and J. SCHLIPF, *Mater. Sci. and Techn.* **12** (1996) 391.
17. A. I. PSHENICHNYUK, V. V. ASTANIN and O. A. KAIBYSHEV, *Phil. Mag. A* **77** (1998) 1093
18. T. G. LANGDON, *Mater. Sci. Eng.* **A174** (1994) 225.
19. R. Z. VALIEV and O. A. KAIBYSHEV, *Acta metal.* **31** (1983) 2121.
20. G. A. SALISHCHEV, R. M. GALEJEV and R. M. IMAYEV, in "Superplasticity in Advanced Materials," edited by

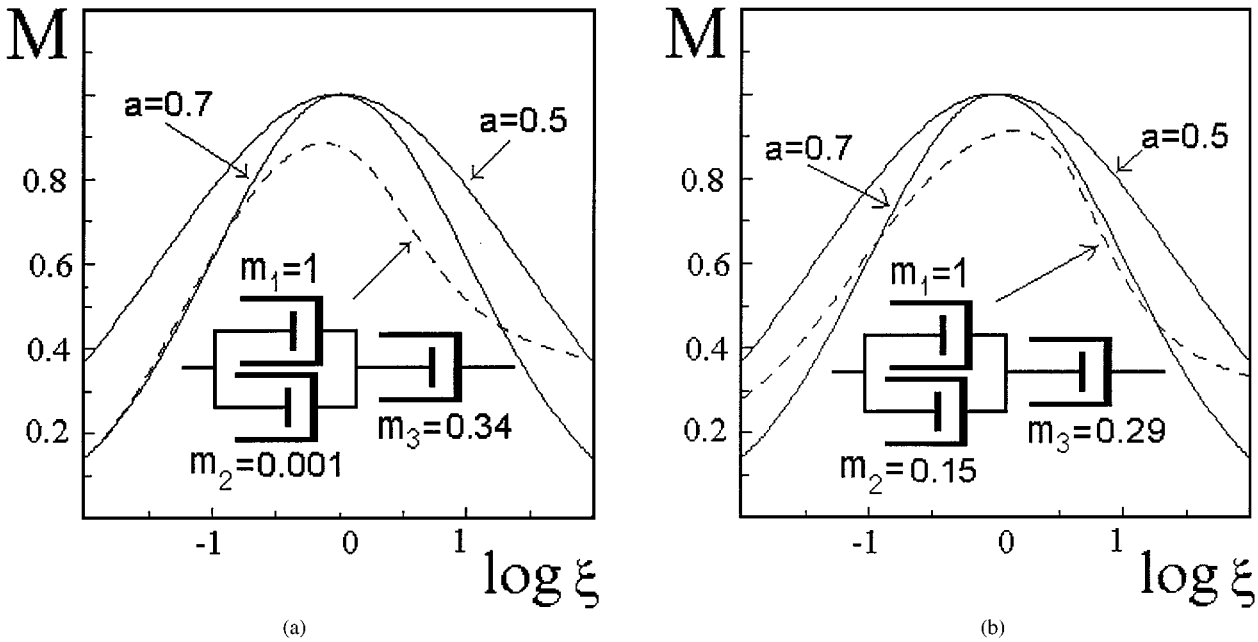

Figure 11 Strain rate dependencies of M-values for universal superplastic curves (solid lines) calculated according to Equation 6 with $M_{max} = 1$ and two different values of a (indicated by the numbers near the curve) and corresponding M—$\log\xi$ dependencies for mixed mechanical model (dashed lines) calculated in accordance with Equations 20 and 21 with different sets of material constants calculated in accordance with Equation 21 with two different sets of material constants: (a) $m_1 = 1$; $m_2 = 0.001$; $m_3 = 0.34$ $\alpha_{10} = 0.94$; $\beta_{10} = 0.96$ $(\Delta = 0.08)$; (b) $m_1 = 1$; $m_2 = 0.15$; $m_3 = 0.29$ $\alpha_{10} = 0.9$; $\beta_{10} = 0.995$ $(\Delta = 0.10)$.

S. Hori, M. Tokizane and N. Furushiro (The Japan Society for Research on Superplasticity, 1991) p. 163.
21. P. L. BLACKWELL and P. S. BATE, *Metall. Trans. A* **24A** (1993) 1085.
22. V. S. LEVCHENKO, V. K. PORTNOY and I. I. NOVIKOV, Unusal low grain boundary sliding in aluminium alloy with classical features of micrograin superplasticity. In: Hori, S., Tokizane, M., Furushiro, N., eds. (1991): Superplasticity in Advanced Materials, ICSAM-91, JSRS, Osaka, Japan, 1991, pp. 39–44.
23. P. L. BLACKWELL and P. S. BATE, *Metall. Trans. A* **27A** (1996) 3747.
24. M. I. MAZURSKI and F. U. ENIKEEV, *Physica Status Solidi* **206** (1998) 519.
25. A. A. SIRENKO, M. A. MURZINOVA, F. U. ENIKEEV, *J. of Mater. Sci. Letters* **14** (1995) 773.
26. R. M. IMAYEV and V. M. IMAYEV, *Scripta Metallurgica* **25** (1991) 2041.
27. N. G. ZARIPOV, O. A. KAIBYSHEV and O. M. KOLNOGOROV, *Phys. Solids* **35** (1993) 2114 (in Russian).
28. N. G. ZARIPOV, O. A. KAIBYSHEV, L. V. PETROVA and O. YU. EFIMOV, *J. Mater. Sci. Letters* **12** (1993) 502.
29. H. IWASAKI, K. HIGASHI, S. TAHIMURA, T. KOMATUBARA and S. HAYAMI, in "Proc. Int. Conf., Superplasticity in Advanced Materials," edited by S. Hori, M. Tokizane, N. Furushiro (Jap. Soc. Res. on Superplasticity, Osaka, Japan, 1991) p. 447.
30. A. K. GHOSH and C. H. CHENG, *ibid.* 299.
31. S. L. STONER and A. K. MUKHERJEE, *ibid.* 323.
32. F. H. MOHAMED, *J. Mat. Sci. Ltrs* **7** (1988) 215.
33. G. S. MURTY and S. BANERJEE, *Scripta Metallurgica* **31** (1994) 707.
34. S. W. ZEHR and W. A. BACKOFEN, *Trans. Am. Soc. Metals* **61** (1968) 300.
35. A. K. GHOSH, in "Superplastic Forming of Structural Alloys," edited by N. E. Paton and C. H. Hamilton (Publ. TMS–AIME, Warrendale, Pensylvania, 1982) p. 85.
36. H. E. CLINE and T. H. ALDEN, *Trans AIME* **239** (1967) 710.
37. J. A. MARTIN and W. A. BACKOFEN, *ASM Trans Quart* **60** (1967) 352.
38. F. U. ENIKEEV, K. A. PADMANABHAN and S. S. BHATTACHARYA, *Mater. Sci. Technol.* **15** (1999) 673.
39. R. A. VASIN, F. U. ENIKEEV and M. I. MAZURSKI, in "Proceed. of Int. Sem. on Microstructure, Micromechanics and Processing of Superplastic Materials (IMSP 97), Mie University, Tsu, Japan, 7–9 August 1997," edited by T. Aizawa, K. Higashi and M. Tokuda (Mie University Press) p. 223.

Received 26 April
and accepted 22 October 1999